

ANOMALOUS AERODYNAMIC HEATING OF A DEAD-END CAVITY IN AN ONCOMING FLOW

V. I. Kuznetsov and D. D. Shpakovskii

UDC 534.2

Anomalous aerodynamic heating of a dead-end cavity in an oncoming flow is experimentally studied and discussed. Based on the experimental results, a physical model of the process, i.e., eddy gas flow in the channel of the dead-end cavity with energy transfer from the external flow, and a mathematical model and calculation methods of the process are developed.

Anomalous gas heating in a dead-end cavity is, in essence, the heating of the gas up to a temperature higher than the stagnation temperature of the main flow that cannot be explained by the customary concepts of aerodynamic heating of a body in a steady gas flow. Eliseev and others [1-3] point to the wave nature of the pressure fluctuations obtained and the temperature rise higher than the stagnation temperature in the cavity. Passage of a forward wave and a shock wave reflected from the cavity bottom over the gas column is manifested in intense pressure fluctuations in the cavity and is accompanied by the increase in the stagnation temperature. This theoretical model of the process contradicts the Wulfsberg equation and laws of conservation, according to which the total temperature behind the shock wave does not change. The main goal of the present work is to define the essence of the occurrence of anomalous heating of the dead-end cavity.

Let us consider a scheme of the experiments conducted in [1-3]. Figure 1 shows the layouts of the cavities relative to an oncoming flow and the configuration of the cut of the leading edges of the cavity. In all experiments with different dead-end cavities carried out in different oncoming flows, the main gas flow moved along the axis of the dead-end cavity. The gas entered the cavity parallel to its axis, which with its further retardation and separated flow over the cavity edges resulted in the phenomenon described above. Theoretical calculations for such a physical model are given in [4, 5]; however, the case discussed below is of different nature.

In the experiments described above, the external flow was directed parallel to the axis, with the exception of [1], where the model was blown by the flow at different angles of attack. Consider the process that can occur in flow past the dead-end cavity (Fig. 2). If the flow moves at a tangent to the cavity or, more exactly, in parallel with it, the velocity vector at the cavity inlet will be directed as shown on the left in Fig. 2. This leads to a velocity gradient with a rapid decrease deep into the cavity, which ultimately causes vortex formation in the cavity. On the right in the figure, streamlines are depicted for the cavity with a velocity vector perpendicular to its axis. This classical model problem was considered in [6] for Reynolds numbers ranging from 400 to 2500. As a result, a flow pattern was obtained that differs radically from the wave effect considered above. If the flow scheme depicted in Fig. 2 is implemented, then the process must proceed as follows. Due to viscosity forces the vortex formation and energy transfer from the external flow to the eddy flow are initiated in the cavity. The process of energy transfer leads to an increase in the pressure and temperature of the gas in the cavity embraced by the eddy flow. As the total pressure in the cavity becomes higher at all points than the total pressure at the inlet, the gas undergoes adiabatic expansion. The time when the eddy flow reaches the dead end of the cavity is taken as the beginning of gas outflow from the dead-end cavity. We assume that the cavity is filled with the gas from the static pressure in the external flow up to its total pressure, then the energy is supplied in the form of viscous friction work (actually, both processes can occur simultaneously). Thereafter the gas flows out of the cavity into the external flow until the pressure inside the

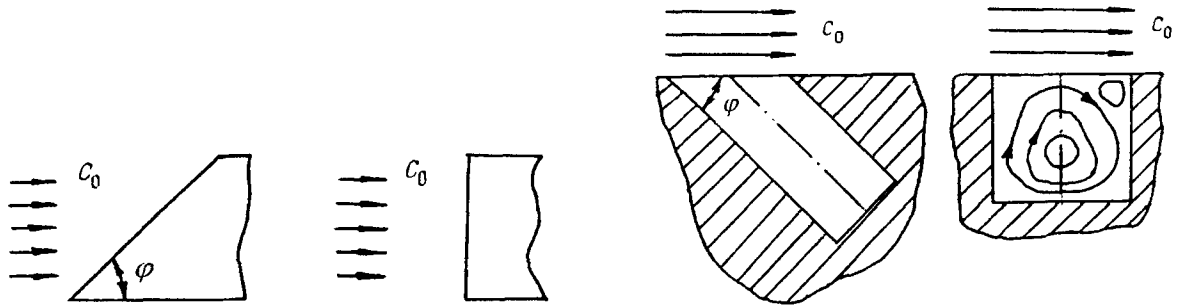


Fig. 1. Schemes of blowing of dead-end cavities with different configurations of their edges.

Fig. 2. Schemes of blowing of the cavity in the experiment and the tentative flow pattern in the cavity.

TABLE 1. Comparison of the Experimental and Calculated Results

Ordinal No.	c_0 , m/sec	T_{01} , K	T_{02} , K	ΔT_{02} , K	P_{01} , Pa	P_{02} , Pa
<i>Experiment</i>						
1	438.26	349.27	372.9	23.6	332825.1	416885.4
2	436.18	345.9	368.3	22.3	332825.1	412758.9
3	437.62	348.2	371.38	23.12	332825.1	415767.8
4	422.1	345.72	365.27	19.54	305887.6	369574.5
5	435.6	348.77	375.46	26.69	328240	422994.8
<i>Calculation</i>						
1	438.26	349.3	378.83	29.56	332825.1	440067.6
2	436.18	345.9	375.16	29.26	332825.1	439694.8
3	437.62	348.2	377.69	29.5	332825.1	439950.3
4	422.1	345.7	373.48	27.7	305887.6	398927.4
5	435.6	348.8	378.03	29.26	328240	433014.7

cavity drops to the static pressure in the main flow stream. Below, the process that occurs is calculated only for the case shown in Fig. 2 or for a similar case.

We carried out a series of experiments with a dead-end cavity of the following geometry: $a = 0.065$ m as its width; $b = 0.013$ m as its height; the angle of inclination of the channel axis of the dead-end cavity toward the plane was $\varphi = 30^\circ$; the channel length of the dead-end cavity along the median axis was $L_d = 0.346$ m. The open end of the dead-end cavity faced the plane blown by the oncoming air flow with different total pressure and stagnation temperature. The air flow moved at a tangent to the plane. In the experiments, measurements were made of the total pressure and stagnation temperature of the external oncoming flow and of the stagnation temperature in the cavity at the base of the dead end. The external oncoming flow was initiated by a screw-type compressor and a nozzle placed on the guiding plane. Results of the experiments with the dead-end cavity are provided in Table 1.

We formulated a mathematical model of the process with the following assumptions:

1. The eddy motion in the channel (Fig. 3) is represented in the form of nonrigid rotating bodies-circumferences, for which the radial distribution of velocities and potential flow are taken into account but the dimensions and configuration of the vortex are ignored assuming that its diameter is equal to the diameter of the channel or its height b ; moreover, its displacement along the channel is not taken into account since its velocity is incommensurably small as compared to rotary motion (from the experiments with vortices).

2. It is assumed that the following modes of energy transfer and conversion participate in the process: a) energy supply in the form of viscous friction work at the inlet of the dead-end cavity; b) conversion of the mechanical energy due to friction in the cavity channel to the internal energy of the gas with an increase in

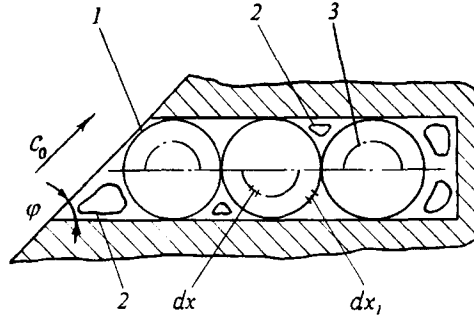


Fig. 3. Physical model of the process: 1) vortex in the form of a nonrigid circumference body; 2) secondary vortices; 3) line indicating the trajectory of flow motion.

the total pressure and temperature. Heat removal through the cavity walls is neglected (the process is assumed to be adiabatic).

3. Neglect of "intermediate" and "secondary" eddy flows (Fig. 3) initiated by the main flows.

4. Friction losses are taken into account in terms of the equivalent diameter and the motion trajectory shown in Fig. 3 by the dash-dot line. It is assumed that the total pressure and temperature extend to the entire volume encompassed by the eddy streams and change at each instant of time.

5. The quantity k does not change.

With allowance for the assumptions made, we write the system of equations describing the process of energy supply into the dead-end cavity:

$$L = \frac{\pi L_d}{2}, \quad dt = \frac{dx}{c_{\text{cir}}}, \quad (M^2 - 1) \frac{1}{c} \frac{dc}{dx_1} = \pm \frac{k}{a_s^2} \frac{dA_{\text{fr.ch}}}{dx_1},$$

$$\frac{T_{0i}}{T_{01}} = \left(\frac{P_{0i}}{P_{01}} \right)^{\frac{k-1}{k}}, \quad A_{\text{fr.i}} = \frac{k}{k-1} RT_{01} \left[\left(\frac{P_{0i}}{P_{01}} \right)^{\frac{k-1}{k}} - 1 \right],$$

$$\frac{P_{0i}}{\rho_{0i}} = RT_{0i}, \quad dA_{\text{fr.ch}} = \xi_{\text{ch}} \frac{dx_1}{d_{\text{eq}}} \frac{c^2}{2}, \quad d_{\text{eq}} = \frac{2ab}{a+b}, \quad (1)$$

$$\xi_{\text{ch}} = \frac{0.3164}{\text{Re}_{\text{ch}}^{0.25}}, \quad \text{Re}_{\text{ch}} = \frac{cd_{\text{eq}}}{\nu_i}, \quad dA_{\text{fr.i}} = \xi \frac{l}{d_{\text{eq}}} \frac{c_0^2}{2},$$

$$\xi = \frac{0.3164}{\text{Re}^{0.25}}, \quad l = c_0 t, \quad \text{Re} = \frac{c_0 d_{\text{eq}}}{\nu_0}, \quad x_1 = x/2.$$

The obtained system of equations (1) is not closed since the kinematic viscosities ν_i and ν_0 for the gas in the cavity and at the cavity inlet are not determined. To determine them, we use the following system of equations:

$$\mu_0 = \mu_{273} \frac{273 + \text{const}_1}{T_1 + \text{const}_1} \left(\frac{T_1}{273} \right)^{3/2}, \quad \nu_0 = \frac{\mu_0}{\rho_1},$$

$$\mu_i = \mu_{273} \frac{273 + \text{const}_1}{T_i + \text{const}_1} \left(\frac{T_i}{273} \right)^{3/2}, \quad \nu_i = \frac{\mu_i}{\rho_i}. \quad (2)$$

In this system of equations ρ_1 , T_1 , ρ_i , and T_i are the static parameters of the gas determined in terms of the calculated stagnation parameters T_{0i} , T_{01} , ρ_{01} , and ρ_{0i} . The velocity i in the system of equations (1) is mean-integral over the cross section, the area of which is $F = ba/2$. Therefore we supplement the systems of equations (1) and (2) with a system of equations describing the circumferential-velocity distribution over the cross section:

$$\begin{aligned} \text{const}_2 &= \frac{c_0}{\left(\frac{b}{2}\right)^2}, \quad h = \frac{b}{2} - \left(\frac{c_{\text{cir}}b}{2 \text{const}_2}\right)^{1/3}, \quad V_{\varphi \text{max}} = \frac{c_{\text{cir}}b}{2\left(\frac{b}{2} - h\right)}, \\ c_{\varphi 1} &= V_{\varphi \text{max}} \frac{\frac{b}{2} - h}{h} \ln \frac{b}{b - 2h}, \quad c_{\varphi 2} = \frac{1}{6} \frac{c_{\text{cir}}b}{\frac{b}{2} - h}, \\ c &= \frac{c_{\varphi 1}h + c_{\varphi 2}\left(\frac{b}{2} - h\right)}{\frac{b}{2}}. \end{aligned} \quad (3)$$

In (3), consideration is given to a half of the channel since the velocity distribution in the second half of the vortex is identical.

The system of equations (3) is constructed on the basis of the relations taken from [7]. For the systems of equations (1)-(3) to become complete, we add the boundary conditions in the form of geometric parameters of the dead-end cavity φ , d_{eq} , and L_d and flow parameters at the dead-end cavity inlet determined from experiment, namely, c_0 , P_{01} , T_{01} , T_1 , and P_1 . As a result, we arrive at a system of the equations describing a time-dependent process. The calculation results are given in Table 1. They differ from the experimental data in the increment in stagnation temperature ΔT_0 by 10–15% and in absolute values of the stagnation temperature T_{02} by no more than 5%.

NOTATION

L , length of the curve circumscribed by the particle moving around the eddy flow periphery; x , current coordinate around the eddy flow periphery; x_1 , current coordinate along the vortex median; d_{eq} , equivalent diameter of the cross section of the dead-end cavity; l , conditional length; h , thickness of the peripheral layer of the vortex with potential flow; F , cross-sectional area; t , current time of the process; c_{cir} , circumferential velocity at the vortex periphery; c , mean integral circumferential velocity over the cross section; c_0 , velocity of the external flow above the inlet to the cavity; a_s , velocity of sound; $c_{\varphi 1}$ and $c_{\varphi 2}$, circumferential vortex velocity in the potential part of flow and in the viscous-flow region; $V_{\varphi \text{max}}$, maximum circumferential velocity of the vortex; T_{01} , stagnation temperature of the oncoming flow; T_{0i} , current stagnation temperature in the cavity; T_i , current static temperature in the cavity; T_1 , static temperature of the oncoming flow; T_{02} , stagnation temperature in the cavity at the end of energy supply; ΔT_0 , absolute increase in the stagnation temperature in the dead-end cavity; P_{01} , total pressure of the oncoming flow; P_{0i} , current total pressure in the cavity; P_1 , static pressure of the oncoming flow; P_{02} , total pressure in the cavity at the end of energy supply; ρ_1 , static density of the oncoming flow; ρ_{01} , density of the retarded oncoming flow; ρ_0 , current static density in the cavity; ρ_{0i} , current density of the retarded flow in the cavity; R , gas constant; $A_{\text{fr.ch}}$, friction work in the channel; $A_{\text{fr},i}$, friction work of the external flow transferred to the gas in the cavity due to viscosity; ν_i , current kinematic viscosity in the cavity; ν_0 , kinematic viscosity of the external flow; μ_i , current dynamic viscosity in the cavity; μ_0 , dynamic viscosity of the external flow; μ_{273} , dynamic viscosity under standard atmospheric conditions; M , Mach

number; k , adiabatic exponent; ξ_{ch} , friction coefficient for the dead-end cavity channel; ξ , friction coefficient for the inlet of the dead-end cavity; Re_{ch} , Reynolds number for the dead-end cavity channel; Re , Reynolds number for the external flow at the dead-end cavity inlet. Subscripts: d, dead-end; eq, equivalent; cir, circumferential; s, sound; fr, friction; ch, channel; max, maximum.

REFERENCES

1. Yu. B. Eliseev and A. Ya. Cherkez, *Mekh. Zhidk. Gaza*, No. 1, 113-119 (1978).
2. V. M. Kuptsov and K. N. Filatov, *Mekh. Zhidk. Gaza*, No. 3, 167-170 (1974).
3. V. M. Kuptsov, *Mekh. Zhidk. Gaza*, No. 5, 104-111 (1977).
4. G. E. Dumnov, *Mekh. Zhidk. Gaza*, No. 4, 177-180 (1977).
5. G. E. Dumnov and G. F. Telenin, *Mekh. Zhidk. Gaza*, No. 4, 173-176 (1977).
6. L. G. Loitsyanskii, *Mechanics of Liquids and Gases* [in Russian], Moscow (1987).
7. V. I. Kuznetsov, *Theory and Calculation of the Rank Effect* [in Russian], Omsk (1995).